International Conference on Geology, Geotechnology and Mineral Resources of Indochina (GEOINDO 2005)
28-30 November 2005, Khon Kaen, Thailand

Paleo-Earthquakes Along The Southern Segment of The Sri-Sawat Fault, Kanchanaburi, Western Thailand:Morphotectonic And TI-Dating Evidence

Rutchut Nuttee
Physics and General Science Program, Faculty of Science, Udon Thani Rajabhat University, Udon Thani, 41000, Thailand.
e-mail: rutchut@chula.com

Punya Charusiri
Associate Professor, corresponding author, Dept. of Geology, Faculty of Science, Chulalongkorn University, 10330, Thailand.
e-mail: cpunya@chula.ac.th

Isao Takashima
Professor
Dept. of Geology, Akita University, 1-1 tegatagakuenn, Akita 010-8502, Japan.

Suwith Kosuwan
Geological Survey Division, Department of Natural Resources and Environments, Bangkok, 10400, Thailand.

ABSTRACT

Kanchanaburi area is selected for paleoseismic investigation due to many earthquakes occurring at various magnitudes for decades. Several major faults in Kanchanaburi area were studies earlier, such as Three Pagodas (TPF), Mae Ping Fault (MPF) and Sri Sawat Faults (SSF). Among these faults, the NW-trending Three Pagodas (TPF) and Sri Sawat Faults (SSF) seem to be the most important faults, cutting through several strata of different lithologies and ages. The Sri-Sawat Fault (SSF), the NNW-SSE trending oblique strike-slip fault with the total length of about 380 km, is located between the Three Pagodas Fault (TPF) and the Mae Ping Fault (MPF). Earthquake swarms and the occurrence of two alarming earthquakes with magnitudes of 5.6 and 5.8 on April 15 and 22, 1983, respectively, are regarded closely related to the SSF.

We selected the southern part of the Sri Sawat Fault (SSF) to clarify the paleoearthquake events, to determine ages of fault movements, and to estimate their slip rates and magnitudes of paleoearthquakes, using remote sensing, field and TL dating investigations.

Our remote-sensing interpretation together with morphotectonic features indicates sharp lineaments, some lineaments cut through the Cenozoic basins. Geologic and geomorphic evidence supports the right-lateral displacement of the studied SSF. Young depositions of sediments are well-observed in several locations nearby the SSF. The offset of topsoil and pediments observed from recent road-cut exposures strongly advocates the local reverse fault movement of the SSF. Therefore, the studied SSF is consequently regarded as the right lateral, reverse fault.

Seven representative quartz-rich samples of colluvial sediments related to the SSF from the excavated trench at Kaeng Khaep and eleven samples from trenches at Pha Tawan were collected for thermoluminescence (TL) dating using total bleaching method. The geochronological and geological results indicate four faulting events during Quaternary Period; i.e., prior to 80.4 ka, 36.7 to 49.3 ka, 29.5 to 30.0 ka, and 5.8 to 9.2 ka events.

Slip-rates along the studied SSF based on the method of McCalpin (1996) is about 0.672 mm/year, and its magnitude using the surface rupture length described by Wells and Coppersmith (1994) is about 6.3 M_W. Our overall result shows the activeness of the southern SSF within Holocene Epoch.

Keywords: paleo-earthquakes, Sri-Sawat Fault, Kanchanaburi, morphotectonic, Thermoluminescence

1. INTRODUCTION

Thailand, one of the countries in mainland southeast Asia, is located in the intraplate of Eurasian plate. Historic data indicate that there were many major historical earthquakes felt in Thailand (Nutalaya et al., 1985 and Nutalaya, 1992), particularly those in the northern and western parts of the country. An earthquake violent enough to destroy the large ancient city, for example, in 460 A.D., 7th lunar month, 22nd Saturday night – Yonok Nakabandhu, was foundered. The whole town was submerded and become lake. The intensity is approximately XII of MM scale (Nutalaya, 1992). In Thailand, the first seismogram was installed in Chiangmai in 1963 and detect many earthquakes since 1963 till present (Nutalaya, 1992). However, most of them are microseismic and low-magnitude. It is important that the data explained above should be not abandoned because detected seismic distribution from seismograph can confirm us whether or not seismicities still actives in Thailand and concern with densely populated area or mega-construction as reservoir.

Kanchanaburi is located in the western part of Thailand, and there are many earthquakes occurring at various magnitudes for decades (Fig. 1). Several major faults in Kanchanaburi area were studied earlier by Chantarame et al., (1981), Shrestha (1987), Siribhakdi (1987), Chaviroj (1991), Hinthong (1991), Nutalaya (1992), and very recently by Won-In (2000). Among these faults, the NW-trending Three Pagodas (TPF) and Sri Sawat Faults (SSF) seem to be the most important faults, cutting through several strata of different lithologies and ages. This perhaps makes the geological structure and morphology of the concerned area more intricate.

The Sri-Sawat Fault (SSF), the NNW-SSE trending oblique strike-slip fault with the total length of about 380 km, can be traced from southeastern Myanmar into western Thailand. The fault is located between the Three Pagodas Fault (TPF) and the Mae Ping Fault (MPF). Earthquake swarms and the occurrence of two alarming earthquakes with magnitudes of 5.6 and 5.8 on April 15

and 22, 1983, respectively, are regarded closely related to the SSF (Shrestha, 1987).

The purpose of this research is to clarify the paleoearthquakes along the southern segment of the Sri-Sawat fault (SSF). The objectives of this research are (1) to identify paleoearthquake evidences along the southern segment of the SSF, (2) to determine the ages of fault movement in the study area, and (3) to estimate the magnitude and slip-rate of these events.

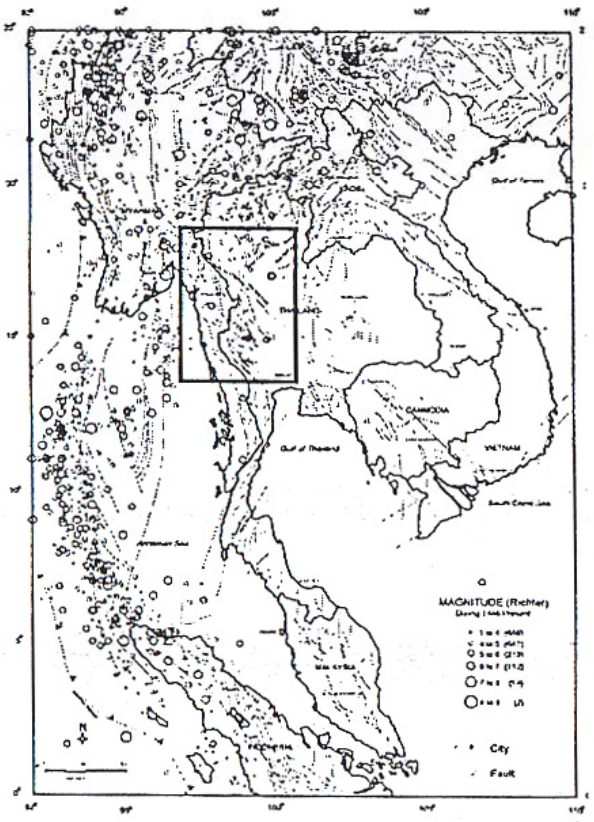

Figure 1. Index map of Thailand and neighboring countries showing epicentral distribution since 1456 to 2000 (Charusiri et al., 2001). Box indicates satellite imagery interpretation in Fig. 2.

2. THE STUDY SITE

The site for paleoseismic study in the current study was selected by morphotectonics and young sediment deposits caused by fault movement using remote sensing interpretation. The satellite imagery Landsat TM5, covering mainly western Thailand and its nearly region, was applied to interpret orientation of three major faults (Fig. 2) in western Thailand including the Mae Ping Fault (MPF), the Sri Sawat Fault (SSF), and the Three Pagodas Fault (TPF).

We infer that the SSF can be separated into three segments base on geologic, seismologic and geomorphologic evidences namely northern, central, and southern segments. The southern segment of the SSF at the south of the Srinagarind Dam is the most interesting fault because it shows very distinct linear trace with abundant morphotectonics features, such as triangular facets, scarps, shutter ridge, and offset streams. Additionally, young sedimentary deposits bound by boundary faults, strongly indicate young faulting. Practically, road-cut and constructions provide many well-preserved exposures.

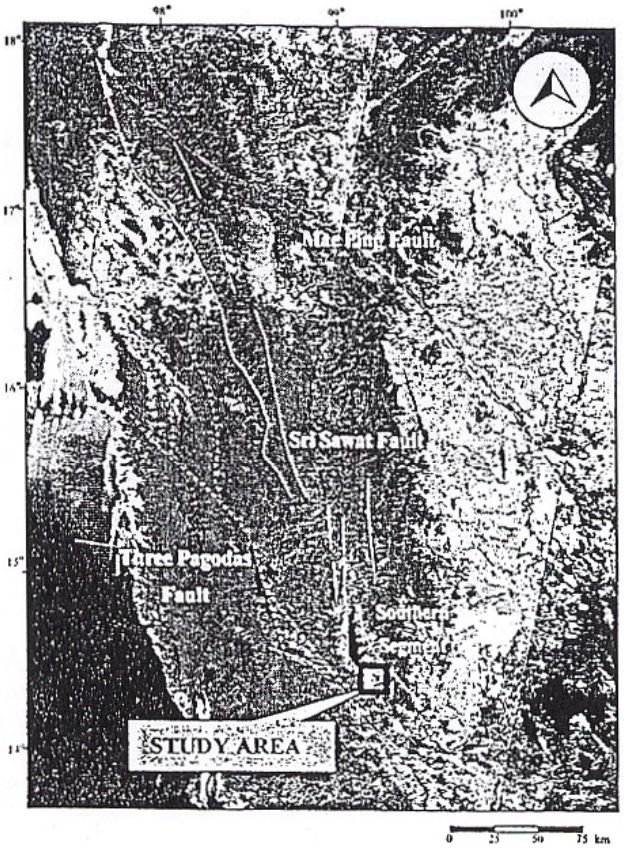

Figure 2. Landsat TM5 satellite imagery showing orientation of three major faults – Mae Ping Fault (MPF), Sri Sawat Fault (SSF), and Three Pagodas Fault (TPF) in western part of Thailand and eastern part of Myanmar

Based on detailed aerial photographic interpretation in the southern segment of the SSF, the study site at Kaeng Khaep area (90 km^2) (Fig.3) shows the very clear and prominent fault in the N50°W trend with well-defined morphotectonic features; such as sets of triangular facets, offset streams, shutter ridges, and young sediment deposits along the fault boundary. This fault can be traced about 12 km long. Detailed geomorphic features were studied by Songmaung (2001).

3. GEOLOGICAL BACKGROUND

3.1 Geological Setting

Geologically, The SSF in the study area cuts through four major rock units (Fig. 4) ranging in age from Cambrian to Triassic. The oldest rock unit in the study area is the Tarutao Group of Cambrian age.

Cambrian Quartzite (C) is the oldest rock unit in the study area. This rock unit mainly includes massive white ortho-quartzite and bedded feldspartic-rich meta-sandstone. Its regional trend is in the NW direction following the major regional structure.

Ordovician Limestone (O) was observed mostly in northeastern part of the area. It mainly includes banded argillaceous limestone and argillite with cephalopods.

Permian Limestone (P) consists of mainly massive and bedded limestone containing fusulined, brachiopads, pelecypods and bryozoans. This unit appears in southern part of the study area.

Triassic Mudstone (TR) consists of mainly shale with Doanella and Halobia; sandstone and interbedded limestone. At Ban Chong Khap and Ban Tha Thong Mon, Posidonia (bivalve fossil), Halobia and Doanella were identified as middle Triassic in age (Bunopas, 1981). This rock unit appears between Cambrian Quartzite and Permian Limestone in the middle and southeast of the study area (Fig.4).

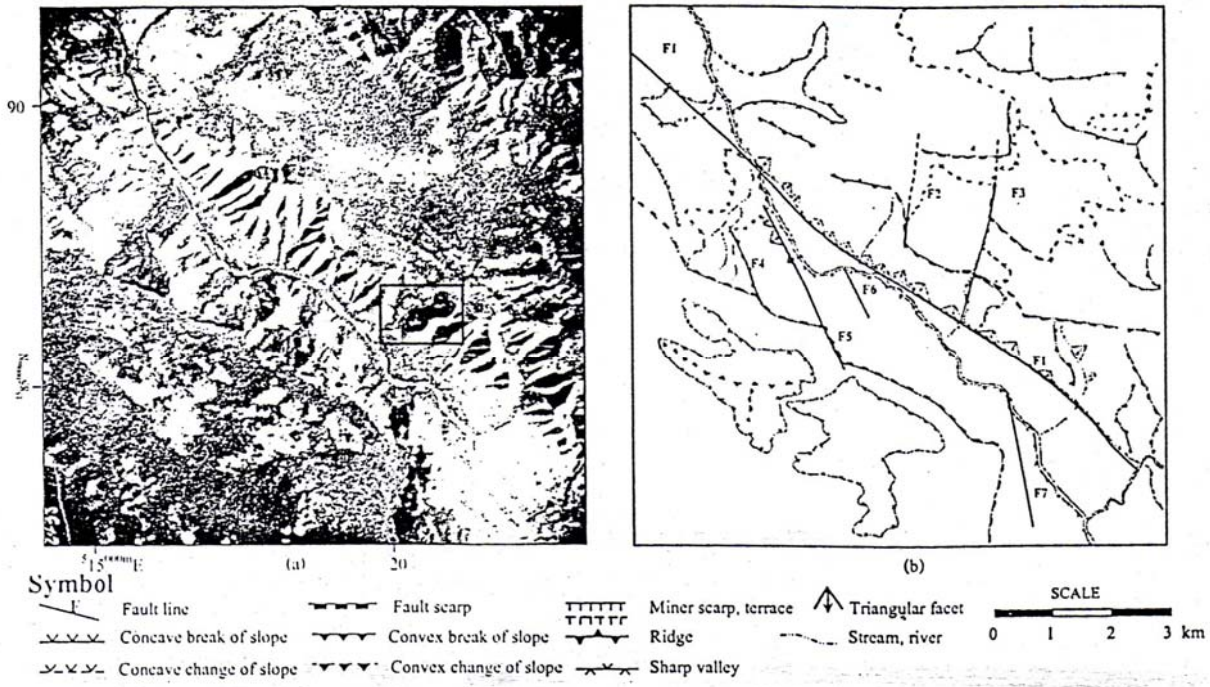

Figure 3. (a) Aerial photographic interpretation of rock distribution, and (b) Morphotectonic interpretation of the similar area.

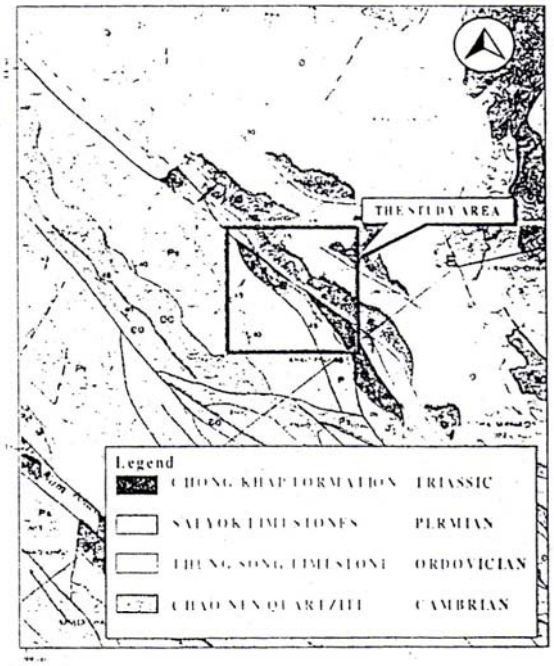

Figure 4. Geological map of the study area and its vicinity showing very deformed and faulted strata of Precambrian to Quaternary ages (after Bunopas, 1976).

3.2 Structural Setting

Faulting

Several faults in this study area and vicinity have been discovered and mostly they are in the NW-SE direction concurring with topographic features of this area (Chantaramee et. al., 1981; Won-In, 2000; Fig.4). Regionally, major faults in the area are not much intricate, except changing of fault direction. The change of fault directions is within the range of 30° from the main strike (N50°W). Therefore, faults seem to lie in the same direction, suggesting that they may have occurred in the same tectonic event. Three kinds of faults are observed viz. strike-slip faults (with oblique components), reverse fault, and normal faults. The first category seems to be much more abundant.

Folding

In Kanchanaburi area, mostly fold axises are the NW-SE trending (Bunopas, 1976; Siribhakdi et al., 1976; Sripongpan and Kojedee, 1987; Kemlek et al., 1989). Fold structures can be recognized in several rocks with many tectonic characters such as synclinal and anticlinal folds (Bunopas, 1976; and Chantaramee et al., 1981). However, difference of form and attitude of fold depend chiefly on characteristic and thickness of rocks. Common attitudes of fold axises are mainly parallel the NW- trending major faults (Chantaramee et al., 1981).

4. METHODS

Methodology of this research is divided into four parts including; data preparation, fieldwork investigation, laboratory analysis, and discussion and conclusion.

The first part starts from gathering to preparing information.The interpretation of remote sensing satellite imagery and epicentral distribution data were used to investigate and locate major faults in western Thailand. The aerial photographic interpretation was used for detailed study in southern segment of Sri Sawat fault.

The fieldwork investigation commences after selecting the study area, and consists of morphotectonic investigation, surveying in the interested area, and trenching. Excavation of trenches leads to the detailed study of subsurface faults and collecting samples for dating of fault movements. After we collected samples, thermoluminescence (TL-) dating technique is the most important part in the laboratory analysis in order to know date of samples and compared to age of faulting.

Then, all of results were complied and analyzed in the final part to prove the deformation from faulting, identification of paleoearthquakes, behavior of fault movement, ages and magnitudes of faulting and possibility of active fault.

4.1 Field Investigation

Detailed field investigation is the best way for studying characteristics of faults and related structural features. In this study, we concentrate our field survey along the southern segment of the SSF. Unconsolidated to semiconsolidated talus deposits with high angular clasts and poor sorting are recognized in some layers. The deposits are interpreted to relate with faulting. In addition, the vertical offset of topsoil and pediments about 1.2 m observed from the recent road-cut exposures at the northern part of the fault, strongly supports the local reverse faulting of the SSF. Furthermore, our morphotectonic analysis using offset stream configuration, at the central part of this fault, indicates right-lateral displacement (Fig.5). In this area, we made a detailed survey for mophotectonic study. We observed that the displacement of offset stream is about 54 m.

4.2 Trenching, mapping and description

We mapped log-stratigraphy at three trench sites herein namely Kaeng Khaep, Pha Tawan I, and Pha Tawan II for detailed studies of faults and description of trench logging. Kaeng Khaep Trench was excavated on young sediment deposits and crossed the interpreted fault trace perpendicularly, near the offset stream. Pha Tawan I and II trenches are abandoned quarries excavated through Triassic clastics by villagers for road/building construction. Although two trenches at Pha Tawan did not cut cross fault trace, they show colluvial deposit closely related to fault movement.

4.2.1 Kaeng Khaep Trench

Kaeng Khaep trench was selected and excavated for its stratigraphic log and detailed study for the southern segment of the SSF. Trench location was defined near the offset stream. It was about 20 m long, 2 m wide, and 4 m deep, covers and almost perpendicular to the fault trace. We recognized 8 horizontal stratigraphic units in an decending order below (Fig.6).

Unit 1 Topsoil or disturbed soil. This unit is the topsoil layer with thickness varying from 6 to 40 cm and averaging 20 cm. It is yellowish brown and poorly sorted. Due to the unit lies at the topmost, it is definitely disturbed by human and agricultural activities.

Unit 2 Chocolate brown colluvium. This unit is the uppermost colluvium in this trench and composed mainly of coarse gravel (80% by volume) support by chocolate brown silty-clayey matrix (about 20%). The colluvium is chocolate brown in color, with thickness varying from 5 to 55 cm and averaging 40 cm. Most fragments are very angular quartzite and feldspar-rich sandstone (av. 1-5 cm in diameter). This unit is interpreted as the youngest colluvial layer in the trench.

Unit 3 Red Colluvium. This colluvium is different from the overlying chocolate brown colluvium (Unit 2) by its lithology and color. It is poorly sorted and mainly comprises coarse to medium gravels. Fragments are generally smaller in size than those of 2 unit and include quartzite and feldspar-rich sandstone with high angularity, and 1 to 3 cm diameter. The matrix consists largely orangish red of fine sand and silt. The shape of the red colluvium with a sharp contact with the underlying unit lead us to regard the red colluvium as a colluvium wedge related to a fault movement.

Unit 4 Brown Colluvium. This unit is poorly sorted and mainly coarse sand to gravel. Fragments are essentially very weathered, yellowish brown, subrounded to angular mudstone with diameter ranging from 0.1 to 1.0 cm. Matrix consists of yellowish brown to brown silt and clay. Due to the similarity in texture and lithology to the underlying unit, it is probably derived from nearby bedrock by "in situ" weathering. This brown layer unit is regarded as the oldest colluvial unit in the trench.

Unit 5 Interbedded red siltstone/mudstone. This unit is strongly weathered mudstone interbedded with siltstone. It is the uppermost bedrock with the average thickness of 150 cm. It shows orangish red to red color probably from oxidation process. The unit regarded as the youngest bedrock unit.Unit 6 Interbedded brown siltstone/mudstone. Beneath the Unit 5 is the brown mudstone interbeded with siltstone. The unit varies in thickness from 15 to 130 cm and averaging about 70 cm. Its textures and lithologies are similar to those of the Unit 5. The unit is characterized by brown to deep brown colors due to less weathering process.Unit 7 Bedrock with white veins/veinlets. This unit is represented by brown to dark brown mudstone interbeded with yellowish brown siltstone layer. The thickness of the Unit 7 exposed varies from 136 to 206 cm with the average of 160 cm. This unit contains steeply inclined to vertical veins and veinlets composed almost entirely of calcite. However, these carbonate veins and veinlets disappear in the overlying Units 5 and 6. The veins/veinlets are vary in thickness about 0.5 to 12 cm. We consider that Unit 7 is separated by the overlying Unit 6, either by a irregular fault contact.

Unit 8 Clay-rich mud. The Unit 8 is located within the Unit 7. The Unit 8 is observed only at the west-side trenching wall and is characterized by very fine-grained, black sediments with somewhat high plasticity. Its shape of this unit is almost ovoid to subrounded and its diameter is about 25 cm. The unit is interpreted to be an excavation due to animals as their dwellings.

Seven samples were collected from the sediments or colluvium units. Four samples were collected from the western wall of trench, and three samples were collected from the eastern wall.

Unit 7 Bedrock with white veins/veinlets. This unit is represented by brown to dark brown mudstone interbeded with yellowish brown siltstone layer. The thickness of the Unit 7 exposed varies from 136 to 206 cm with the average of 160 cm. This unit contains steeply inclined to vertical veins and veinlets composed almost entirely of calcite. However, these carbonate veins and veinlets disappear in the overlying Units 5 and 6. The veins/veinlets are vary in thickness about 0.5 to 12 cm. We consider that Unit 7 is separated by the overlying Unit 6, either by a irregular fault contact.

Unit 8 Clay-rich mud. The Unit 8 is located within the Unit 7. The Unit 8 is observed only at the west-side trenching wall and is characterized by very fine-grained, black sediments with somewhat high plasticity. Its shape of this unit is almost ovoid to subrounded and its diameter is about 25 cm. The unit is interpreted to be an excavation due to animals as their dwellings.

Seven samples were collected from the sediments or colluvium units. Four samples were collected from the western wall of trench, and three samples were collected from the eastern wall.

4.2.2 Pha Tawan I Trench

The Ban Pha Tawan I Trench is an abandoned quarry with the length of 8 m and the width of 4 m.

The study site consists of 8 recognizable horizontal sediment layers of colluvial deposits with interbedded coarse- and fine-grained materials (Fig.7). These colluvium layers are considered to have occurred during times of fault-related earthquakes tranquility, and they deposited near foots of tectonically active slopes. The deposit adjacent to fault scarp is commonly divided into debris and wash facies (similar to those described by Wallace, 1977; Nelson, 1987). The coarse-grained colluviums are regarded as "*debris facies*" that are poorly sorted and composed chiefly of boulder- to pebble-size clasts. Most of the clasts are quartzite and feldspar-rich sandstone with high angularity, suggesting that they were rapidly deposited primary by gravity-controlled process. We therefore consider that blocks and clasts can be released from the exposed fault-free face during activity period by falling and slumping (see Fig.7). On the other hand, the fine-grained layer comprises largely medium to fine sand to silty clay, deposited relatively slowly by surface wash processes, called "*wash facies*". They are inferred to have occurred during the periods of slope stability between faulting events.

In this area, the interbedded sequence of coarse- and fine-grained sediments which displayed almost similar thickness of layer shows cycles of tectonic activity-controlling sequence of fault movements. It is therefore interpreted that eight young unconsolidated sediment layers of alternated coarse- (debris) and fine- (wash) facies may represent four faulting - triggering earthquake events. As also noted by Songmuang (2001), a series of erosional benches in the study area also advocated multiple episodes of earthquake fault movements.

At the Pha Tawan I trench, we collected nine samples for age determination by thermoluminescence dating. All of them were collected in colluvium unit (see Fig.7).

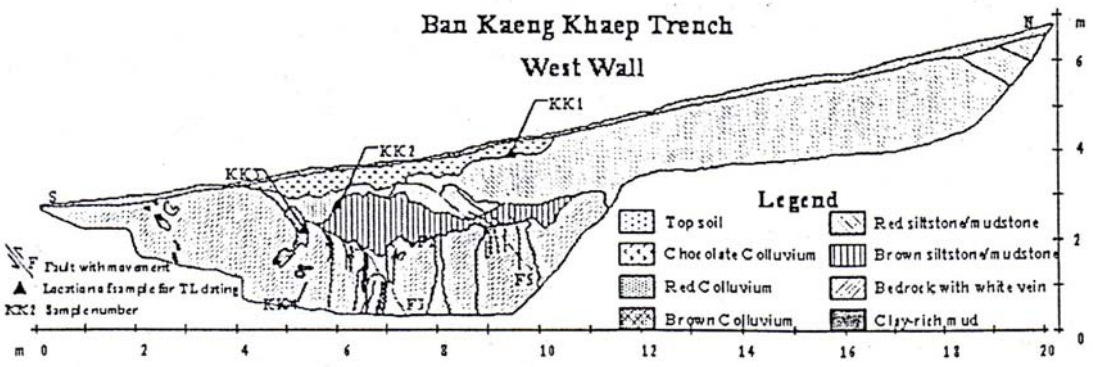

Figure 6. Trench log in the west wall of Ban Kaeng Khaep Trench, showing principle stratigraphy and sample location for TL-dating.

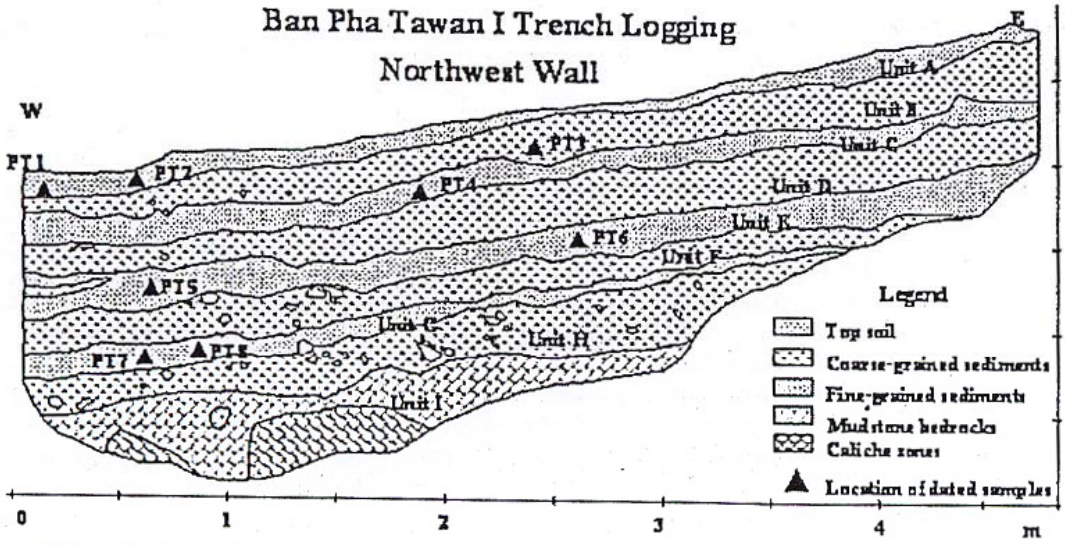

Figure 7. Trench-log sketch map of Ban Pha Tawan I Trench showing principle stratigraphy and sample location for TL-dating.

4.2.3 Pha Tawan II Trench

Pha Tawan II Trench, was dug by villagers for road and building construction. It is situated at about 200 m northwest from Pha Tawan I Trench. The mappable unit exposed in northwest wall was defined into 3 units as shown below.

Unit A. This unit is the uppermost layer in this area. The unit is 10-15 cm thick, dark grey to black soil. It is poorly sorted and comprises mainly coarse gravels about 50%. Clasts are mostly coarse gravels of very angular yellowish to grayish brown quartzite. Clasts diameter is about 1 to 7 cm. The matrix comprises of silt and clay. It is covered by many trees on surface.

Unit B. This unit is orangish red, coarse-grained unconsolidated colluvium, with thickness ranging 0.5-3.0 m. It is poorly sorted and consists mainly of coarse gravels about 85% coarse gravels and gravels are mostly highly angular pale yellow to brown quartzite with diameter of about 3 to 15 cm. Matrix is mainly orangish red silt and clay. The Unit B is covered and shows a graditional contact with the dark grey topsoil and a sharp contact with the underlying bedrocks.

Unit C. This unit is weathered bedrocks of Triassic clastics comprising mainly brown mudstone with interbedded yellow siltstone. This unit exposes about 0.5-3.5 m thick. The structure in this unit is tight folds with axial planes dipping to SW. In some part, the folds change abruptly in their structural attitudes due to faulting. Furthermore, in the middle part of the trench side, the contact between the Unit B-gravel bed with the Unit C-bedrock shows step-like uplifts of the gravel bed and a colluvial wedges, possibly indicating to the effect of earthquake-related tectonic activity.

Only one sample was collected in the coarse-grained colluvium layer (Unit B) for age determination by thermoluminescence dating.

5. THERMOLUMINESCENCE AGE ESTIMATES

Eighteen samples were collected from three trenches for age determination. No organic matter for ^{14}C dating was found in the trenches; therefore all of samples from the trenches were dated using the thermoluminescence (TL-) dating method. This method directly dates silicate mineral grains in sediment, the age reflecting the time since the sediment grains were last exposed to sunlight (Wintle and Hunley, 1980; Forman et al., 1991). TL-dating is, in effect, a radiation microdosimetry of natural settings, and the requirement is to measure the radiation dose provided by natural radioactivity (^{238}U, ^{232}Th and ^{40}K) to minerals. Natural ubiquitous minerals such as quartz, feldspars, zircons, have good TL properties which enable them to record irradiation received by them, and of preserving this record through geologic time. Natural radioactivity constitutes a source of constant radiation to these minerals. In a first approximation, the dose rate can be assumed constant through time (though substantial deviations can occur) (Aitken, 1967; Singhvi and Wagner, 1986).

The TL age equation (Eq.1) in its simplest form is:

$$Age(years) = \frac{Total\ accumulated\ irradiation\ dose\ (Gy)}{Irradiation\ dose\ per\ year\ (Gy/year)\ (AD)} \quad (1)$$

- Total accumulated irradiation dose, or irradiation dose received by natural radioactivity and of preserving this record through geologic time, is called *paleodose* (PD). Irradiation dose per year, or dose rate is called *annual dose* (AD). The annual dose was determined by calculation of natural radioactive elements (U, Th, K) in natural sample. These radioactive elements were detected by gamma ray spectrometry at Akita University, Japan (by Isao Takashima). Annual doses were calculated by the equation derived from Bell (1979) and Aitken (1985)

$$AD = \frac{(01148U+0.0514Th+0.02069K)}{(1+0.14\,Wt.)} + \frac{(0.1462U+0.0286Th+0.6893K)B+0.15}{(1+1.25\,Wt.)} \quad (2)$$

where U = concentration of uranium in ppm, Th = concentration of uranium in ppm, K = concentration of potassium oxide (%), B = beta dose attenuation in quartz grains, and Wt. = Water content (%/100)

Results of U, Th, and K analyses and calculated annual dose are shown in table 1.

In the current study, all of samples for TL-dating method were collected from fault-related colluvial sediments. Quartz grains betweem 74 and 250 μm in diameter were separated from individual samples collected. The samples for TL dating were prepared following the method descrided by Takashima and Watanabe (1994) (see detailed in Nuttee, 2002).

The simplest approach to the evaluation of the total accumulated irradiation dose is by the straight-forward procedure of measuring the natural TL from a portion of quartz grain and comparing it with the artificial TL from that same portion of grain after resetting TL signal to zero and exposure to known dosage of radiation (29, 99, and 289 Gy were used in the current study) from the radioisotope gamma ray source at Akita Hospital, Japan. The dose is given in gray (1 Gy = 100 rad). One gray corresponds to one joule of absorbed energy per kg of matter. TL intensity of natural sample and heated samples with additive dose were measured and shown as "glow curve" (Fig.8) where the x-axis is temperature (in °C) and the y-axis is TL signal (in A.U. (arbitrary unit))

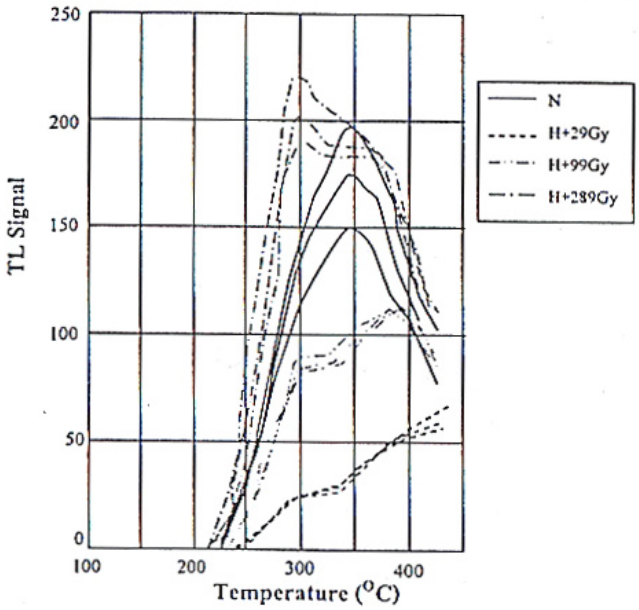

Figure 8. TL glow curve of sample no.KK5, showing TL intensities of natural TL (N) and intensities of gamma-ray irradiated at 29, 99, and 289 Gy (H+□). Each sample was treated in 3 times.

The total accumulated irradiation dose was obtained using the ratio of intensity of gamma ray irradiated (H+□) / intensity of natural (N), for plotting the growth curve (Fig.9). However, in case of sediments, total accumulated irradiation dose cannot be used for TL-age equation as Eq.1. Because resetting of the TL signal by sunlight is less efficient than by heat (Rodbell et al., 1997). Sunlight does not completely empty the trapped electron to zero (Wintle and Huntley, 1980; Aitken, 1985; Huntley, 1985).

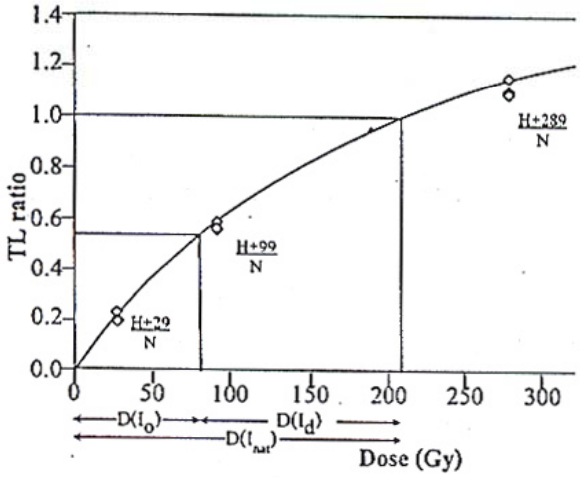

Figure 9. TL growth curve of sample no.KK5, the ratio of intensity of gamma-ray irradiated (H+□) / intensity of natural (N) were plotted. The horizontal line of y-intercept = 1 (which mean $(I_{nat}) / (I_{nat})$) were drawn into the curve, then the line drawn straight down to the x-intercept on x-axis. The value on x-intercept point is total accumulated dose of natural sample $[D(I_{nat})]$ or paleodose. The ratio of $Io/Av.(I_{nat})$ was plotted on y-axis. Then, the accumulated dose after deposit $[D(I_d)]$ was computed by the $[D(I_{nat})]$, was subtracted by $D(I_o)$.

In the current study, each sample was exposed to 8 hr sunlight for resetting of TL signal to residual (inherited) TL level (see detailed in Nutthee, 2002). The TL remaning after bleaching $[D(I_o)]$, or residual TL dose, was determined and plot on curve (Fig.9) for evaluating the accumulated irradiation dose of sediment after deposit $[D(I_d)]$. The accumulated dose after deposit was used to calculate the age of sample as PD in Eq.1. TL data and age estimates of samples were shown in table 2.

5.1 TL Dating results of the Kaeng Khaep Trench

This trench consists of three sedimentary units from top to bottom as chocolate brown colluvium, red colluvium, and brown sediment. Interpretation of TL age results is shown below.

Chocolate colluvium. The corrected dates of this unit from sample no. KK1 in the west trenching wall and KK5 in the east trenching wall, are 30.010 □ 4.22 and 37.445 □ 4.11 ka, respectively. So, the age of this unit is about 30.010 □ 4.22 to 37.445 □ 4.11 ka.

Red colluvium. The corrected dates of this unit as determined from sample no. KK2 in the west trenching wall, and KK6 and KK7 in the east trenching wall, are 80.424 □ 13.09, 77.048 □ 11.25, and 273.727 □ 50.32 ka, respectively. The date of sample KK7 is very old and

Table 1. Results of water content, natural radioactive content (U, Th, K_2O) and annual for TL dating samples from Ban Kaeng Khaep and Ban Pha Tawan I and II Trench.

Sample No.	Water content	U (ppm)	Th (ppm)	K_2O (%)	Annual Dose
Ban Kaeng Khaep Trench					
KK1[a]	13.834	1.048	13.387	3.416	3.441
KK2	12.593	1.468	11.702	2.422	2.768
KK3	11.945	1.491	10.480	2.149	2.522
KK4	13.743	1.397	11.425	2.292	2.602
KK5	10.991	1.332	13.182	3.266	3.512
KK6	11.107	0.988	10.328	2.529	2.714
KK7	10.393	1.631	13.153	2.256	2.851
Ban Pha Tawan I Trench					
PT1[b]	11.018	2.089	15.628	2.096	2.968
PT2	15.155	1.933	13.175	1.661	2.327
PT3	7.515	1.891	15.361	2.048	3.010
PT4	7.528	2.088	15.139	2.037	3.028
PT5	8.334	1.900	14.898	1.939	2.867
PT6	12.160	2.155	14.735	1.845	2.700
PT7	9.263	2.062	17.060	2.104	3.132
PT8	9.765	1.937	15.318	1.846	2.780
PT9	4.582	1.589	15.222	2.921	3.740
PT10	10.852	2.027	15.689	2.547	3.297
Ban Pha Tawan II Trench					
PT11	11.677	1.469	18.717	3.047	3.702

[a]KK1 = Number of samples that collected from Ban Kaeng Khaep Trench

[b]PT1 = Number of samples that collected from Ban Pha Tawan Trench

Table 2 Age estimates for samples from Ban Kaeng Khaep and Ban Pha

Sample No.	Ann. Dose (mGy/y)	$D(I_{nat})$[a] (Gy)	Apparent Age[b] (Ka)	$D(I_o)$[c] (Gy)	$D(I_d)$[d] (Gy)	Corrected Age[e] (Ka)
Ban Kaeng Khaep Trench						
KK1	3.441	159.836	46.444 ± 6.53	56.557	103.279	30.010 ± 4.22
KK2	2.768	467.281	168.841 ± 27.48	244.701	222.581	80.424 ± 13.09
KK3	2.522	211.309	83.798 ± 13.51	120.517	90.792	36.005 ± 5.81
KK4	2.602	126.614	48.668 ± 9.40	37.480	89.134	34.261 ± 6.03
KK5	3.512	209.371	59.618 ± 6.55	77.868	131.503	37.445 ± 4.11
KK6	2.714	571.035	210.409 ± 30.73	361.931	209.104	77.048 ± 11.25
KK7	2.851	1085.718	380.758 ± 70.00	305.195	780.523	273.727 ± 50.32
Ban Pha Tawan I Trench						
PT1	2.968	88.850	29.934 ± 4.32	59.776	29.074	9.795 ± 1.41
PT2	2.327	19.526	8.390 ± 1.08	19.016	0.510	0.219 ± 0.03
PT3	3.010	100.321	33.332 ± 4.57	83.013	17.308	5.751 ± 0.79
PT4	3.028	95.254	31.459 ± 3.76	67.430	27.823	9.189 ± 1.10
PT5	2.867	183.094	63.870 ± 9.64	91.228	91.866	32.046 ± 4.90
PT6	2.700	184.296	68.264 ± 9.61	85.333	98.963	36.656 ± 5.16
PT7	3.132	230.380	73.547 ± 11.87	130.696	99.684	31.823 ± 5.14
PT8	2.780	242.814	87.349 ± 12.26	105.684	137.130	49.331 ± 6.93
PT9	3.740	302.423	80.862 ± 10.40	187.076	115.347	30.842 ± 3.97
PT10	3.297	229.808	69.706 ± 9.94	163.782	66.026	20.027 ± 2.85
Ban Pha Tawan II Trench						
PT11	3.702	405.394	109.499 ± 13.40	296.266	109.129	29.476 ± 3.61

[a]$D(I_{nat})$ = Total accumulated dose or natural dose

[b]Apparent age = TL age estimate before the correction of sedimentary samples

[c]D(Io) = Residual TL dose

[d]D(Id) = Accumulated dose after deposit

[e]Corrected age = TL age estimate after the correction of sedimentary samples

probably regarded fictitious when compared with those of the KK2 and KK6 in the same unit. Beside, this unit shows loosely compacted sediment which indicates to young deposit. We therefore regard the date of 273.727 ka is too old for this unit. For this unit we infer the age of this unit being around 77.048 □ 11.25 to 80.424 □ 13.09 ka.

Brown sediment. This unit was found only in the west wall. The corrected date of this unit was determined from sample no. KK3 is 36.005 □ 5.81 ka. The date is younger than that of the upper unit. We consider this sediment as catacomb of insects, as ants and termites. So this unit was disturbed by bioturbation from overlying layers. The other corrected date is from sample no. KK4 which is 34.261 □ 6.03 ka. This sample was collected from black mud ball that penetrates in bedrock containing calcite veins/veinlets. The date is younger than that of the upper unit.

5.2 TL-Daing results of the Ban Pha Tawan I Trench

Northwest Trenching Wall

Layer A. This unit is a topsoil layer of mostly fine-grained sediment. The corrected ages determined from sample nos. PT1 and PT2 are 9.795 □ 1.41 and 0.219 □ 0.03 ka, respectively.

Layer B. This unit is coarse-grained colluvium. The collected date was determined from sample no. PT3 is 5.751 □ 0.79 ka.

Layer C. This unit is fine-grained colluvium. The collected dates were determined from sample no. PT4. The date of this layer is about 9.189 □ 1.10 ka.

Layer E. This unit is fine-grained colluvium. The collected dates were determined from sample no. PT5 and PT6, and TL dates of this layer are about 32.046 □ 4.90 to 36.656 □ 5.16 ka, respectively.

Layer G. This unit is fine-grained colluvium. The collected dates were determined from sample no. PT7 and PT8, and TL dates of this layer are about 31.823 ± 5.14 to 49.331 ± 6.93 ka, respectively. The 31.823 ± 5.14 ka of sample PT7 is younger than upper units, due to analytical errors.

Southeast Trenching Wall

The sediment in this area is coarse-grained colluvium showing structureless feature. The corrected dates of this unit were determined from sample nos. PT9 and PT10. The date of this colluvium is about 20.027 ± 2.85 to 30.842 ± 2.85 ka, respectively.

5.3 TL-Dating results of the Ban Pha Tawan II Trench

The sediment in this area is coarse-grained colluvium. The corrected date of this unit was determined from sample no. PT11. The age of this colluvium is about 29.476 ± 3.61 ka.

6. DISCUSSION

In this study, all available information and results obtained from the previous chapters are used for discussing behavior of faults, sequence of fault movement, ages of fault movement, and estimation of slip rate and earthquake magnitude of the southern of the Sri Sawat Fault (SSF).

6.1 Behavior of Ancient Movement

The aerial photograph interpretation in the study area together with that of Songmuang (2001) supports that the southern segment of SSF is estimated to be as long as 11 km with the N50°W trend. The support for this part of the SSF is displayed by sharp lineaments, young sedimentation and several clear morphotectonic features. Well-defined fault scarps, sets of triangular facets, offset steams and shutter-ridges, advocate the youthfulness of the fault.

Wang Masang Mt., show four steps of erosional benches supporting multiple episodes of fault movement in the past. Khaep Trench, which shows a contact between bedrock without calcite veins/veinlets (Unit 6) and bedrocks containing these veins/veinlets (Unit 7), is reverse faulting. Consequently, this fault is regarded as the oblique slip fault shown as a block diagram in Fig.10.

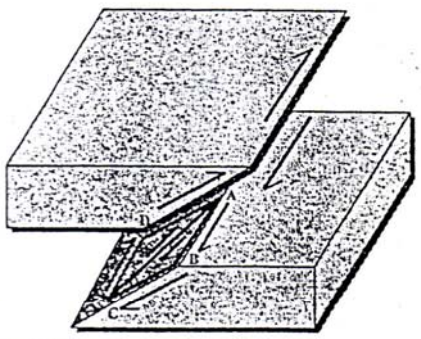

Figure 10. Schematic of oblique slip movement (A-C) of southern segment of SSF.

The offset streams along the 11 km-long of southern SSF indicate that this fault shows right-lateral displacement and the distance of offset stream measured by our detailed survey is about 54 m. Furthermore, the offset of topsoil and pediments about 1.2 m observed from the recent road-cut exposures strongly indicates the local reverse faulting of the SSF. In addition, the fault in Kaeng

However, 1.2 m of vertical movement is quite short compared with 54 m of horizontal movement. Therefore the right-lateral movement is the major component of this oblique-slip fault movement.

6.2 Sequence of Fault Movements

The colluvial deposition in Pha Tawan I Trench shows stratigraphy of eight alternated sedimentary layers of colluviums with coarse- and fine-grained interbeds. Four poor-sorting layers with highly angular fragments (or talus) suggesting rapid deposition provide good evidence for "debris facies" due to possibly 4 earthquake movements. On the contrary, four fine-grained layer composed mostly silty sand to clay suggest low-energy and slow deposition by surface wash processes during the untectonic period. These low-energy layers were inferred to occur during the periods of slope stability between the faulting events. Therefore, this alternating sequence of coarse- and fine-grained colluvium layers is inferred to represent four episodes of past faulting earthquake.

The aerial interpretation of the southern segment of SSF shows the escarpment comprises a series of triangular faceted spurs (Fig.11a) interrupted by several benches (Fig. 11b) and erosional pediment remnants (Fenton et al., 1997). Hamblin (1976) has shown that such features were the result of episodic fault movement. These facets were formed during periods of fault movement and the benches may have formed during periods of tectonic stability, erosion and fault scarp retreat (Fig.11c). The erosional benches along this fault, especially around Khao

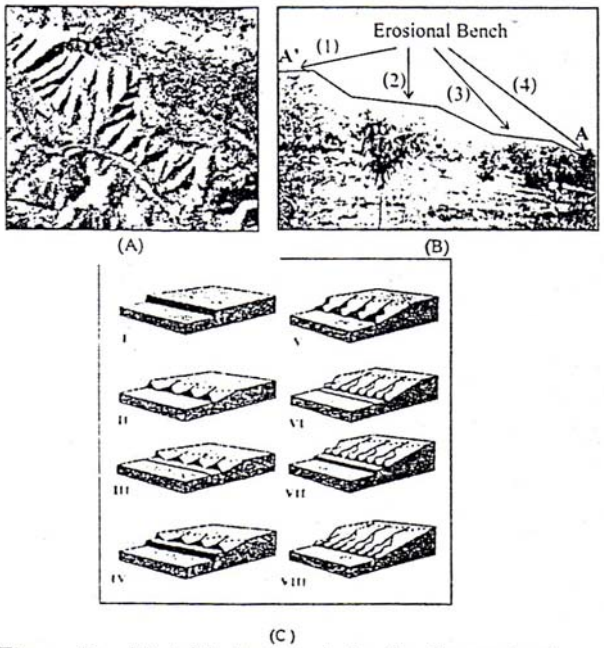

Figure 11. (a) Arial photograph showing the erosional bench in study area. A-A' is a line of cross section through Khao Wang Masang Mt.

(b) A cross-section along the A-A' line in Fig. 14a showing 4 steps of erosional benches in Khao Wang Masang Mt.

(c) Shematic showing stepts of fault movement which produce the erosional bench (Hamblin, 1976).

6.3 Constraint on Earthquake Events

In this current study, all TL-dated samples were collected from fault-related colluviums on trenching walls, i.e., Kaeng Khaep Trench, Pha Tawan I Trench, and Pha Tawan II Trench.

At Kaeng Khaep trench, two sedimentary units were considered for ages of faulting; i.e., red colluvium and chocolate colluvium (Fig. 12). The red colluvium shows wedge-shaped body deposited following faulting event. Similar situation occurred for the colluvium wedges deposited in trenches excavated across fault scarps on the Weber Segment of the Wasatch Fault Zone by Forman et al. (1991). The dates of fault-related red colluvium wedge which are the oldest dates, therefore, indicate the first earthquake faulting may have occurred immediately prior to deposition of the red colluvium. We consider that the age of this faulting might be little older than that of red colluvium more than 80.4 ka B.P. The occurrence of coarse-grained gravels in unit H at Pha Tawan trench (Fig.7) supports this fault activity. No sample was collected for TL age activity in this unit.

After red-colluvial deposition, the fault may have re-activated during 36.0-77.1 ka B.P. as evidenced by the appearance of the chocolate coarse-fragment colluvium deposited over the red colluvium. This chocolate colluvium with 30.2-36.8 ka date corresponds to the unit E with 32.1-36.7 ka date in Pha Tawan I trench. The second faulting may have occurred before deposition of the chocolate colluvium and the Unit E but after deposition of red colluvium. This faulting is responsible for the deposition of coarse-grained gravels (Unit F) without any confirmation of TL dating. So, the second faulting should have occured between 36.7-49.3 ka B.P.

Moreover, we found that the wedge-shaped body in chocolate colluvium layer, corresponding to Unit E in Pha Tawan I Trench, were cut by fault. So, this subsequent faulting may have occurred after deposition of the chocolate colluvium (and the Unit E) but before that of 9.2 ka of Unit C. The third faulting may have caused deposition of the undated Unit D. However, the sediment

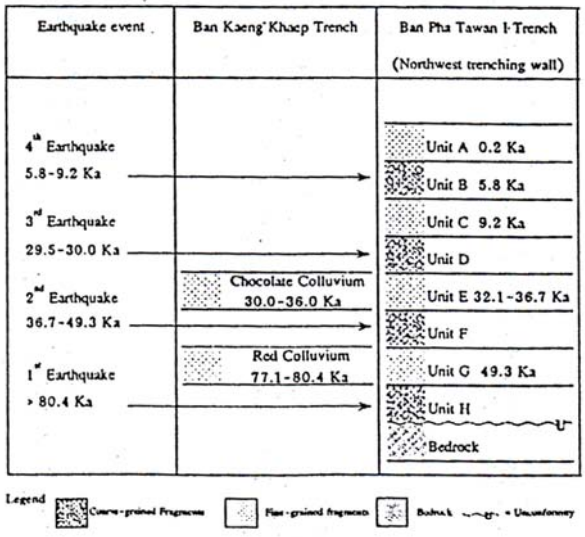

Figure 12. Schematic showing event of earthquakes and their ages; considered by stratigraphy and TL age dating result of Ban Kaeng Khaep Thench, Ban Pha Tawan I Trench.

of Unit D is regarded equivalent to the gravel layer on southeast trenching wall in Pha Tawan I Trench with the dates of 20.0-30.8 ka. Moreover, the presence of the 29.5 ka of gravel layer in Pha Tawan II Trench provides a good support for this earthquake event. So, the third earthquake faulting may have taken place between 29.5-30.0 ka B.P.

The debris sediments of Unit B, probably occurred by earthquake activity, deposited during 5.8 ka B.P. So, the latest (fourth) earthquake may have triggered (after the Unit C but before the Unit B) during 5.8 and 9.2 ka B.P.

6.4 Calculation of Fault Slip Rate

Fault slip rate is the rate of slip on the fault averaging over a time period involving several large earthquakes (Yeast et al., 1997). The slip rate is calculated from the cumulative displacement of dated landforms or deposits. A good example for such slip rate calculation is that of the Pajarito fault of northern New Mexico (McCalpin, 1995). However, calculation of slip rate does not require recognition or dating of any individual paleoearthquakes (McCalpin, 1996). In this study, the cumulative displacement was measured from the offset of stream by detailed survey; viz about 54 m, due to 1.2 m of vertical displacement in recent road-cut exposure is little, compare with 54 m of horizontal displacement and no another location to shows better vertical displacement. In addition, the erosional process may affect decrement of fault displacement, which exposed on ground surface. Therefore, the slip rate is not true displacement. Small numbers of paleoearthquakes characterized on the southern SSF constrains our ability to access the variability of slip rates over the time span for the studied SSF. Due to Holocene geologic setting, a slip rate on this investigated fault can only be calculated from cumulative displacement on the 80.4 ka-old datum. A mean long-term slip rate of 0.67 mm/yr was computed. Confirmation is also supported by the work of Shrestha (1987) who estimated the average slip rate of the SSF by using empirical relations established between earthquake magnitude and seismic source parameters at about 0.73 mm/yr.

6.5 Estimating Paleoearthquake Magnitude

Although various types of primary evidence have been used to infer magnitudes for paleoearthquakes, the length of the surface rupture and maximum displacement on continental fault traces are by far the most commonly used parameter (Bonilla et al., 1984; Wells and Coppersmith, 1994). The inferred rupture length and slip for paleoearthquakes are compared to worldwide data on rupture length and slip during historic earthquakes (of known magnitude) to estimate a probable paleoearthquake magnitude (McCalpin, 1996). Dating precision and accuracy of stratigraphic and geomorphic correlation play the important roles in magnitude estimation. This is between paleoearthquakes closely spaced in time may have created surface features that appear to the product of one large paleoearthquake after thousand years (see McCalpin, 1996). Moreover, two sources of uncertainties exist in the SRL method as noted by Bonilla et al. (1984), and Fumal et al. (1993). The first source is from deficiencies in the lengths cited in the historical data set, and the second source is by difficult in accurately measuring the length of prehistoric ruptures.

Paleoearthquake magnitudes have traditionally been estimated from primary fault-zone evidence (surface

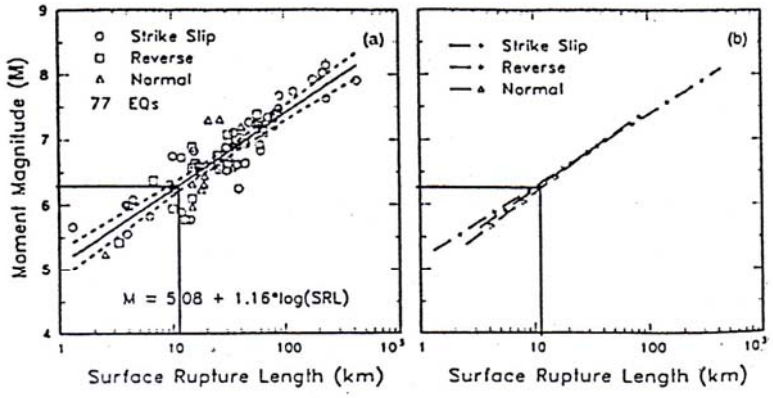

Figure 13. A paleo-earthquake of the southern segment of the SSF is estimated at about 6.3 M using SRL of 11 km. (a) Surface rupture length (SRL, in km) as a function of moment magnitude (M) for 77 earthquakes in the historic data set of Wells and Coppersmith (1994). Equation at bottom lists regression of M on log SRL for all fault types. Note that in part (b) there is a little difference between the relationships for the three fault types.

rupture length or displacement), rather than from secondary ground-shaking evidence. The earlier approach was to compare the inferred rupture length (L) or maximum displacement (D) from a paleoearthquake with the corresponding measurements from historic earthquakes of known magnitude.

Surface rupture length method of paleomagnitude estimate involves estimating the length of prehistoric surface rupture, and comparing its length to the surface rupture lengths (SRLs) of historic earthquakes of known magnitude. The most recently analyzed historic data set for this comparison is that of Wells and Coppersmith (1994), although similar plots are presented by Slemmons (1982), Bonilla et al. (1984), Heaton et al. (1986), and Khromovskikh (1989). Wells and Coppersmith's regression of surface rupture length on moment magnitude (M_W) for 77 worldwide earthquakes of all slip type is shown in Fig.13. The historical data range from M_W 5.8 to 8.1. Although, regression may be made for different styles of faulting (strike-slip, thrust, or normal), Wells and Coppersmith (1994) concluded that the difference were not large.

In this study, the equation for all fault types was used for estimating a paleoearthquake magnitude of the southern segment of the SSF.

$$M = 5.08 + 1.16 \log(SRL) \qquad (3)$$

Where M is Moment magnitude (M_W)
SRL is Surface rupture length (km)

Base on the Landsat TM5 imagery and aerial photograph interpretation, the length of the studied southern segment of the SSF is about 11 km. Therefore, the paleoearthquake magnitude is about 6.29 M_W.

7. CONCLUSIONS

Base on our study, conclusions can be drawn for the southern segment of the Sri Sawat Fault as follows;

1. The southern segment of the SSF is about 11 km long. Behavior of this segment shows oblique strike slip movement with the right lateral and reverse components.

2. Geochronological results together with morphotectonic and structural field analyses point to the four events of past earthquake faulting; i.e., the prior to 80.4 ka, the 36.7 to 49.3 ka, the 29.5 to 30.0 ka and 5.8 to 9.2 ka events.

3. The studied southern segment of the SSF is regarded as the active fault because the last faulting event occurred during a period of 11,000 years (Holocene time).

4. The measurement of offset stream and TL age results, allows calculating an average slip rate, based on method described by McCalpin (1996), to be about 0.672 mm/year.

5. The fault length of 11 km indicates the surface rupturing of paleoearthquakes on the southern segment of the SSF, based on method described by Wells and Coppersmith (1994), to be M_W magnitudes of 6.3.

However, the paleoseismology of the SSF should be more studied in the future for ascertainment of data and information. The good paleoseismic data is necessary for seismic hazard assessments in this area. Moreover, the age of faulting should be considered and relied on more samples, and other dating methods that will be obtained.

Nevertheless, the present study indicates, though a low chance, that this fault is considered to be of interest, regarding that large associated earthquakes possibly occur in the future.

8. ACKNOWLEDGEMENTS

Grateful acknowledgements are made to Electricity Generating Authority of Thailand, Ministry of Educational Affair, and Thailand Research Fund (TRF) for financial supports.

The authors are highly indebted to Krit Won-In of the Research Institute of Materials and Resources, Akita University, for his beneficial comment onTL-dating equipment and results.

Thanks are also to Preecha Saithong of the Geological Survey Division, Department of Mineral Resources (DMR), for his encouragements and providing all the necessary research facilities and to Naramase Teerarungsigul and Santi Sri-chum for detailed survey facilities.

9. REFERENCES

Aitken, M.J., 1967. Thermoluminesce. *Science Journal* 1: 32-38.

Aitken, M. J. 1985. *Thermoluminescence Dating*. London: Academic.

Bell, W. T. 1979. Thermoluminescence dating: Radiation dose-rate data. *Archaeometry* 21: 243-245.

Bonilla, M. G., Mark, R. K., and Lienkaemper, J. J. 1984. Statistical relation among earthquake magnitude, surface rupture length, and surface fault displacement. *Bulletin of the Seismological Society of America* 74: 2379-2411.

Bunopas, S. 1976. Geology of map Changwat Suphan Buri, Sheet ND 47-7, Scale 1:250,000. *Report of*

Investigation, Number 16, Volume 1 and 2. Geologic map and text. Bangkok : Department of mineral Resources.

Bunopas, S. 1981. Paleogeographic history of western Thailand and adjacent part of southeast Asia: A plate tectonic interpretation. Doctoral dissertation, Graduate School, Victoria University of Wellington.

Chantaramee, S., Thanadpipat, C., Wattanikorn, K., Hararak, M., and Jitapunkul, S. 1981. *Tectonic pattern of west and northwest Thailand (in Thai)*. Unpublished report prepared for National Research Council of Thailand: Bangkok.

Chuaviroj, S. 1991. *Geotectonic of Thailand (in Thai)*. Bangkok: Geological Survey Division, Department of Mineral Resources.

Fenton, C.H., Charusiri, P., Hinthong, C., Lumjuan, A., and Mangkonkarn, B., 1997. Late Quaternary fault in northern Thailand. *The International Conference on Stratigraphy and Tectonic Evolution of Southeast Asia and South Pacific.* Bangkok, Department of Mineral Resources, August 19 - 24: 436 -452.

Formam, S.L., Nelson, A.R., and McCalpin, J.P. 1991. Thermoluminescence dating of faulting-Scarp-derived colluvium: Deciphering the timing of paleoearthquake on the Weber Segment of the Wasatch fault zone, North Central Utah. *Journal of Geophysical Research* 96: 595-605.

Fumal, T. E., Pezzopane, S. K., Weldon, R. J., II, and Schwartz, D. P. 1993. A 100-year average recurrence interval for San Andreas fault at Wrightwood, California. *Science* 259, 199-203.

Heaton, T.H., Tajima, F., and Mori, A. W. 1986. Estimating ground motions using recorded accelerograms. *Survey Geophysics*. 8:25-83.

Hamblin W.K. 1967. Patterns of displacement along the Wasatch fault. *Geology* 4: 619-622.

Hinthong, C., 1991. Role of tectonic setting in earthquake events in Thailand, In *ASEAN-EC Workshop on Geology and Geophysics*, pp. 1-37. Jakarta: Indonesia.

Huntley, D. J. 1985. On the zeroing of the thermoluminescence of sediments. *Physics and Chemistry of Minerals* 12: 122-127.

Kemlek, S., and Jeamton, S., and Angkhajan, V. 1989. Geology of Amphoe Thong Pha Phum, Ban I-tong. And Khao Ro Rae, with geological map scale 1:50,000, sheet 4738 III and 4738 IV (in Thai). Bangkok: Department of Mineral Resources.

Khromovskikh, D. S. 1989. Determination of magnitudes of ancient earthquakes from dimension of observed seismodislocations. Tectonophysics 166: 1-12.

McCalpin, J.P. 1995. Frequency distribution of geologically-determined slip rates for normal faults in the western USA. *Bulletin of the Seismological Society o Americ* 85. 867-1872.

McCalpin, J.P.(ed.) 1996. *Paleoseismology*. San-Diago: Academic.

Nelson, A. R. 1987. A facies model of colluvial sedimentation adjacent to a single-event normal fault scarp, Basin and Range province, western United states; Directions in Paleoseismology: *United States Geological Survey Open File Report* 87-673: 136-145.

Nutalaya, P. 1992. Crustal stability and seismic hazards in Thailand. In *Proceeding of a National Conference on Geologic Resources* of Thailand: Potential for Future Development, pp.s2-1 – s2-20. Bangkok: Thailand.

Nutalaya. P., Sodsri, S., and Arnold, E. P. 1985. Series on Seismology Volume II-Thailand: Southeast Asia Association of Seismology and Earthquakes Engineering, 403 p.

Nuttee. R., 2002. Young Faulting along the southern segment of Sri Sawat Fault. Changwat Kanchanaburi. Master's Thesis, Department of Geology, Graduate School, Chulalongkorn University, Bangkok.

Rodbell, D.T., Forman S.L., Pierson, J., and Lynn, W.C. 1997. Stratigraphy and chronology of Mississippi Valley loess in western Tennessee. *GSA Bulletin* 109: 1134-1148.

Shreatha, P. M. 1987. Investigation of Active Fault in Kanchanaburi Province, Thailand. Master's Thesis. Graduate school, Asian Institute of Technology.

Singhvi, A.K., and Wagner, G.A. 1986. Thermoluminescence dating and its applications to young sedimentary deposits. In A.J. Hurford, E. Jager, and J.A.M.Ten Cate (eds.), *Dating Young Sediments: Proceeding of the Workshop, Beijing*, pp. 159-190. Bangkok: CCOP Technical Secretarial.

Siribhakdi, K. 1987. Seismogenic of Thailand and periphery. In P. Lukunaprasit, K. Chandrangru, S. Poobrasert, and M. Mahasuverachai (eds.), *Proceeding of the 1st Workshop on Earthquake Engineering and Hazard Mitigation*, p.151-158. November 1986. Bangkok: Chulalongkorn University.

Siribhakdi, K., Salyapongse, S., and Sutheeron, V. 1976. *Geological map of Tavoy, scale 1:250,000, sheet ND47-6*. Bangkok: Geologic Survey Division, Department of mineral Resources.

Slemmons, D. B. 1982. Determination of design earthquakes magnitudes for microzonation. In Proc. Third Int. Earthquake Microzon. Conf., Seattle, WA; *Earthquake Engineering Research Institute* 1: 110-130.

Sripongpan, P., and Kojedee, T. 1987. Geology of Ban Tha Ma dua, Khao Bo Ngam, Ban Phung and Ban Lin Thin with geological map scale 1:50,000, sheet 4738 IV, 4738 I, 4838 IV and 4838 IV (in Thai). Bangkok: Geologic Survey Division, Department of mineral Resources.

Takashima, I., and Watanabe, K. 1994. Thermoluminescence age determination of lava flow/domes and collapsed materials at Unzen

Volcano, SW Japan. Bulletin of Volcanology Society of Japan 1: 1-12.

Wallace, R. E. 1977. Profile and ages of young fault scarps, north-central Nevada. *Bulletin of the Seismological Society of America* 9: 1267-1281.

Wells, D. L. and Coppersmith, K. J. 1994. New empirical relationships among magnitude, rupture length, rupture area, and surface displacement. *Seismological Society of American Bulletin* 84: 974-1002.

Wintle, A.G., and Huntly, D.J. 1980. Thermoluminescence dating of ocean sediments. *Canadian Journal of Earth Science* 17: 348-360.

Won-In, K. 2000. *Neotectonic evidence along the Three Pagoda Fault Zone, Changwat Kanchanaburi.* Master's Thesis, Department of Geology, Graduate School, Chulalongkorn University, Bangkok.

Yeats R. S., Sieh, K., and Allen C. R. 1997. *The geology of earthquakes*. Oxford: Oxford University Press.